



## Removal of reactive dye from textile effluent through submerged filtration using hollow fiber composite nanofiltration membrane

Xueyan Zhu<sup>a</sup>, Yinping Zheng<sup>a</sup>, Ze Chen<sup>a</sup>, Qing Chen<sup>a</sup>, Bijuan Gao<sup>a</sup>, Sanchuan Yu<sup>a,b,c,\*</sup>

<sup>a</sup>Department of Chemistry, Zhejiang Sci-Tech University, Hangzhou 310018, P.R. China

Tel:+86 571 86843217; Fax: +86 571 86843217; emails: yuschn@163.com, lmeih@zstu.edu.cn

<sup>b</sup>Key Laboratory of Advanced Textile Materials and Manufacturing Technology of Education Ministry, Zhejiang Sci-Tech University, Hangzhou 310018, P.R. China

<sup>c</sup>Engineering Research Center for Eco-Dyeing & Finishing of Textiles, Ministry of Education of China, Zhejiang Sci-Tech University, Hangzhou 310018, P.R. China

Received 30 July 2012; Accepted 3 January 2013

---

### ABSTRACT

The removal of reactive dye from textile effluent through submerged nanofiltration (NF) was investigated in this study. The textile effluent containing reactive dye of Reactive Black 5 was treated with a hollow fiber membrane module manufactured from laboratory-fabricated composite NF membranes with a molecular weight cutoff of 760 Da. The submerged NF system was evaluated for dye removal efficiency, permeate flux and permeation resistance as a function of transmembrane pressure (TMP) and volume concentrating factor (VCF). It was found that, under the suction pressure of lower than 1.0 bar, the membrane retained nearly all the dye molecules presented in the textile effluent but retained the electrolytes to a much low extent, so that the submerged filtration system could be operated under low suction pressure. Dye removal efficiency increased with increasing TMP, while permeability decreased with increasing TMP and VCF. Average dye removal rate of higher than 99.8% and steady flux of 5.75 l/m<sup>2</sup>h could be achieved by the submerged NF system operated under the TMP of 0.8 bar and VCF of 4.0. Furthermore, the submerged NF system possessed good antifouling property and high water cleaning efficiency.

*Keywords:* Dye removal; Nanofiltration; Submerged filtration; Hollow fiber nanofiltration membrane; Decolorization

---

### 1. Introduction

The treatment of textile effluents is one of the most significant environmental problems, since most synthetic dyes have complex aromatic molecular structures that make them inert and biodegradable difficult [1–3]. Approaches such as adsorption [4–6], physico-chemical coagulation [7,8], microbial degradation

[9,10], chemical oxidation [11–13] and photochemical degradation [14,15] have been proposed to remove dyes from the textile effluents. However, all of the mentioned methods suffer from one limitation or another, and none have been successful in removing color from textile wastewater completely. Therefore, it is an urgent need to develop decolorization methods that are more effective and suitable for textile industry.

\*Corresponding author.

Membrane technology, as an advanced separation technology, has gained popularity and become a promising technology to treat and reuse wastewater [16]. Recently, the membrane process of nanofiltration (NF) has attracted much attention of environmental scientists and engineers in the removal of dyes from textile wastewater for its unique separation characteristics. For example, Akbari et al. [17] treated the anionic dye solution using hollow fiber NF membrane developed by photografting. It was reported that the tailor fabricated negatively charged hollow fiber membrane with a 4,500 Da molecular weight cut-off could be used to concentrate a saline Direct red 80 solution with a high water permeability of 15.01/h m<sup>2</sup> bar, a high dye rejection of more than 97.0% and a salt retention of lower than 2.0%. Lau et al. [18] reviewed the preparation, performance evaluation, transport modeling and fouling control of polymeric NF membranes for textile dye wastewater treatment. They concluded that NF offers many more advantages compared with conventional treatment methods and the other categories of membrane technologies, and research and development in this field are a must in order to gain confidence in NF for textile wastewater treatment system. Bes-Piá et al. [19] investigated and compared the performance of three NF membranes in treatment of biologically treated textile wastewater. It was reported that all the three tested NF membranes designed as Desal 5 DK, Duraslick, and TFC-SR2 could retain the dyes presented in the effluent and the color of the NF permeates was negligible. The treated effluent with high enough quality could be recycled to the machinery washing processes and print implements. More recently, combined process of coagulation–flocculation and NF was adopted by Ellouze et al. [20] to treat a mixture of effluents coming from different textile industry. It was reported that, with coagulation–flocculation as pretreatment prior to NF, retentions of 57, 100, and 30% could be achieved for COD, color and salinity, respectively, at a volume reduction factor of 3 under optimal pressure and temperature of 10 bar and 40°C. However, these conventional NF processes are generally operated under the model of tangential pressurized filtration, which is commonly associated with the disadvantages of high energy consumption and severe membrane fouling [21].

Therefore, submerged filtration, a filtration model that possesses the advantages of lower energetic consumption and cleaning requirement compared with the tangential pressurized filtration mode [22–24], was adopted in this work to remove reactive dyes from textile wastewater. Dye removal experiments were conducted with real textile effluent containing reactive

dye of Reactive Black 5 employing a laboratory-fabricated hollow fiber composite NF membrane module, which was manufactured from laboratory-fabricated composite NF membranes with a molecular weight cut-off (MWCO) of 760 Da. The treatment efficiency was investigated in terms of dye removal rate and permeate flux under different operating conditions. Additionally, the permeation resistance and membrane cleaning were also investigated.

## 2. Materials and methods

### 2.1. Materials and reagents

The industrial effluent was collected from a textile dye house located in Zhejiang, China. It contains the reactive dye of Reactive Black 5 (a four-valent sodium salt having a molecular weight of 991 g/mol), electrolyte of sodium chloride and other chemical additives such as surfactants. The wastewater was filtrated using microfiltration membrane with a mean pore size of 0.1 µm in diameter to remove the particles and colloids presented in the effluent. The characteristics of the pre-treated textile effluent used in this study are presented in Table 1. The chemical structure of Reactive Black 5 is shown in Fig. 1.

The hollow fiber composite NF membrane with a MWCO of about 760 Da used in this study was prepared in our laboratory by coating the outside of the polypropylene microporous support hollow fiber with a cross-linked sodium carboxymethyl cellulose (CMCNa) selective thin layer using dip-coating technique described in our previous study [25]. The properties of the nanofiltration membrane used are summarized in Table 2. It exhibited relatively lower rejection rates to salts under the testing trans-membrane pressure (TMP) of 0.8 bar when comparing with those values obtained under the higher TMP of 3.0 bar [25].

De-ionized water with a resistivity of 18.0 MΩ was used as pure water. Other chemicals involved were all analytical grade and used without further purification.

Table 1  
Characteristics of the textile effluent used in this study

Parameter	Unit	Value
pH		7.2 ± 0.2
Reactive Black 5	mg/l	32.0 ± 3.0
Conductivity	µs/cm	4,800 ± 200
NaCl	mg/l	2,600 ± 100
Na <sub>2</sub> SO <sub>4</sub>	mg/l	120 ± 20
TSS	mg/l	<1.0

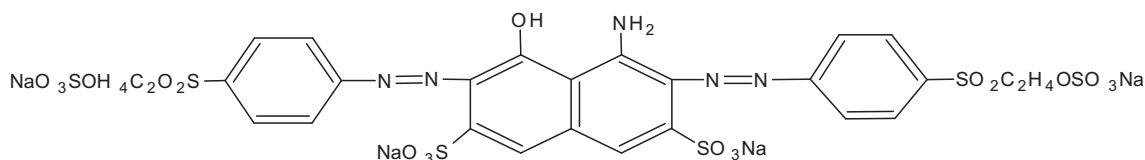


Fig. 1. Chemical structure of Reactive Black 5 presented in the textile effluent.

Table 2  
Properties of the hollow fiber NF membrane used in this study

Parameter	Value
Pure water permeability, <sup>a</sup> $l/m^2$ h bar	$10.8 \pm 0.4$
MWCO, <sup>a</sup> Da	760
Surface zeta potential at pH 7.0, <sup>a</sup> mV	$-3.2 \pm 0.3$
Surface contact angle (SCA), <sup>a</sup> °	79.9
Inner diameter, mm	0.40
Outer diameters, mm	0.50
Rejection rate to NaCl, <sup>b</sup> %	$19.5 \pm 0.5$
Rejection rate to Na <sub>2</sub> SO <sub>4</sub> , <sup>b</sup> %	$68.5 \pm 0.6$

<sup>a</sup>Data obtained from Ref. [25].

<sup>b</sup>Tested with 500 mg/l salt aqueous solution at TMP of 0.8 bar, 25.0°C and pH 7.0.

## 2.2. Filtration setup

The experimental setup for submerged filtration is schematically shown in Fig. 2. It mainly contains a submerged hollow fiber module, a suction pump (with a maximum pressure difference of 0.98 bar), pressure regulator, an aeration unit and a feed tank with a volume of 10.0 l. The hollow fiber NF membrane modules used in this study were made from the above laboratory-fabricated hollow fiber composite NF membranes and potted in the laboratory. Each module contains twenty U-shaped hollow fibers of 25.0 cm length and has an effective outer surface area of 78.6 cm<sup>2</sup>. The submerged NF hollow fiber membrane mod-

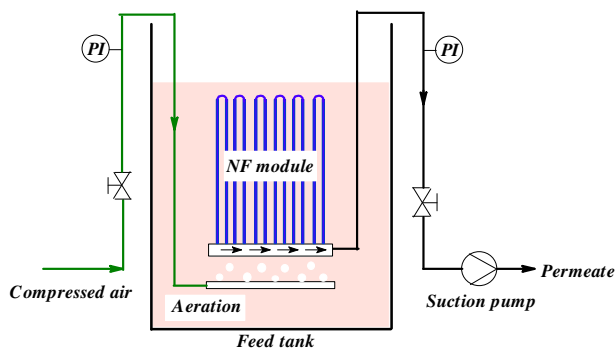


Fig. 2. Experimental setup for submerged NF.

ule was performed in an outside-to-inside mode under a certain TMP (suction pressure) generated by the suction pump. Like in membrane bioreactor (MBR) applications, the membrane module was aerated at a constant flow rate of 1.0 l/min to control the fouling on the membrane.

## 2.3. Submerged filtration tests

Submerged filtration tests were conducted employing the above described experimental setup under constant temperature of 25.0°C. The dye removal rate, permeate flux, membrane fouling and cleaning efficiency of the submerged NF system were investigated under different conditions.

Firstly, the membrane module was pre-filtrated with de-ionized water under 0.8 bar for 2.0 h before test to ensure stable membrane flux. Then, submerged NF tests with the textile effluent were carried out under the circulation mode, under which permeate was recycled into the feed tank to keep the feed composition constant. The filtration tests were conducted by varying the TMP from 0.6 to 0.9 bar. Each filtration test consisted of three steps. For the first 30 min of the test, de-ionized water was used as the feed solution. After the measurement of pure water flux ( $J_{wi}$ ) under a certain TMP, the feed tank was refilled with the textile effluent, and the filtration test was run under the same TMP until a steady flux ( $J_{ws}$ ) was obtained, during which periodical measurements were carried out with the filtration system to check the flux and dye removal rate. After which, the membrane module was washed with flowing de-ionized water for 30 min and the cleaned membrane module was measured for pure water flux ( $J_{wc}$ ).

Finally, submerged filtration tests with the textile effluent were also carried out at the constant TMP of 0.8 bar under concentrating model by withdrawing the permeate from the system during filtration. The system was operated under different volume concentrating factors (VCF, defined as the volume ratio of the initial effluent to the concentrated effluent) to investigate the  $J_{wi}$ ,  $J_{ws}$  and color removal rate. After each run under a certain VCF, the fouled membrane module was washed with flowing de-ionized water for 30 min

and then measured for the pure water permeate flux  $J_{wc}$ .

#### 2.4. Measurements

Average permeate flux was determined by measuring the permeate volume collected over a certain period in terms of liter per square meter per hour ( $l/m^2 h$ ) and calculated according to the following equation:

$$J_w = \frac{V}{A \times \Delta t} \quad (1)$$

where  $J_v$  is the volumetric average permeate water flux,  $A$  is the effective area of the membrane for permeation, and  $V$  is the volume of permeate over a time interval  $\Delta t$ .

The observed average dye removal rate was calculated using the following equation:

$$R_{dye} (\%) = \frac{C_f - C_p}{C_f} \times 100 \quad (2)$$

in which  $C_f$  and  $C_p$  represent the dye concentrations in the feed and permeate, respectively, which were measured using an ultraviolet–visible spectrophotometer (UV759, Shanghai) at the maximal absorption wavelength of 592 nm for dye Reactive Black 5.

The observed average salinity retention rate was calculated using the following equation:

$$R_{salinity} (\%) = 1 - \frac{\text{Conductivity}_p}{\text{Conductivity}_f} \times 100 \quad (3)$$

where  $\text{Conductivity}_f$  and  $\text{Conductivity}_p$  represent the salinity of the feed and permeate, respectively, which were measured by a conductance meter (DDSJ-308A, Cany Precision Instruments Co. Ltd, China).

### 3. Results and discussion

#### 3.1. Salinity retention

The salinity retention of the submerged system in filtration the textile wastewater was investigated through conductivity measurement. Fig. 3 presents the time-dependent conductivity of the permeate and feed streams and the average salinity retention when the system was operated under the circulation model at the constant TMP of 0.8 bar. What is apparent from the graph is that, during the whole filtration period of 40 h, the feed conductivity lies between 4,750 and 4,830  $\mu s/cm$ , while the permeate conductivity varies

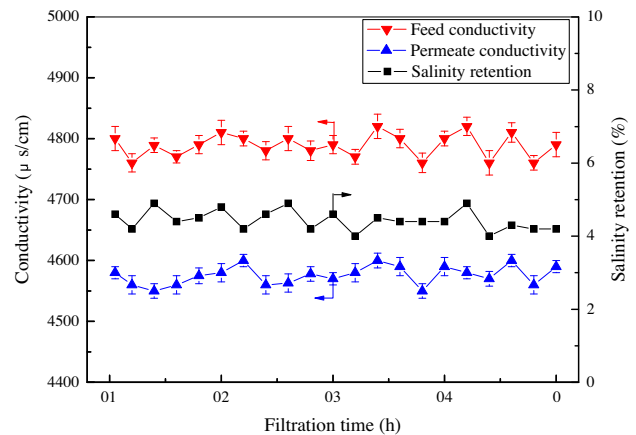


Fig. 3. Changes of the permeate conductivity ( $\blacktriangle$ ), feed conductivity ( $\blacktriangledown$ ) and observed salinity retention ( $\blacksquare$ ) with filtration time for the submerged NF system filtrated with textile wastewater under circulation model at TMP of 0.8 bar and 25.0°C

slightly and lies in a range from about 4,550 to 4,600  $\mu s/cm$ . The observed average salinity retention rate, as shown in the figure is about 4.5%, indicating that the NF membrane used retains salts presented in the feed textile effluent to a little extent and electrolytes will not accumulate in the feed tank. Therefore, the submerged NF system can be operated under comparable low suction pressures similar to those of ultrafiltration modules in MBR.

#### 3.2. Dye removal

Dye removal efficiency of the submerged NF system in treatment of textile wastewater was investigated by measuring the contents of Reactive black 5 in permeate and feed under different conditions.

Fig. 4 presents the change of the observed average dye removal rate with filtration time for the submerged NF system operated under circulation model at the TMP of 0.8 bar. It is apparent that, as the filtration time prolongs, the observed average dye removal rate ascends and then reaches to a steady value after 30 h. The increase of dye removal rate with filtration time may be explained in terms of both the steric hindrance and Donnan exclusion effects that mainly determining the retention rate of NF membrane to charged solutes [26]. The adsorption of the anionic dye molecules on the membrane surface will enhance the membrane negative charge, thereby enhancing the Donnan exclusion effect. On the other hand, the adsorption of dye molecules onto the inner surface of membrane pores during filtration will result in a reduction in mean pore size of the membrane used, thereby increasing the steric hindrance effect [27].

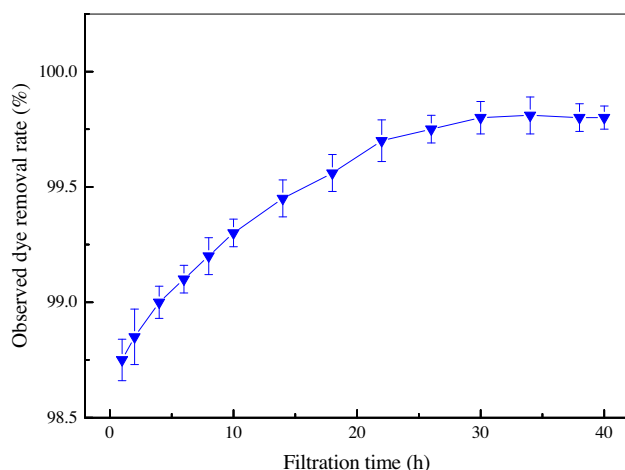


Fig. 4. Change of the observed average color removal rate with filtration time for the submerged NF system filtrated with textile effluent under circulation model at the TMP of 0.8 bar and 25.0°C.

The steady observed dye removal rates under different TMPs are presented in Fig. 5, which clearly shows that the steady observed dye removal rate varies slightly when the TMP increases from 0.6 to 0.9 bar, showing a value of higher than 99.5%. The results indicate that high removal efficiency of the dye reactive black 5 can be achieved through submerged filtration using a NF membrane with a MWCO of about 760 Da even under a relatively low TMP of 0.6 bar.

Table 3 presents the steady observed average dye removal rates under different VCFs. Under the TMP of 0.8 bar, with the increasing VCF, the observed average dye removal rate of the submerged NF system

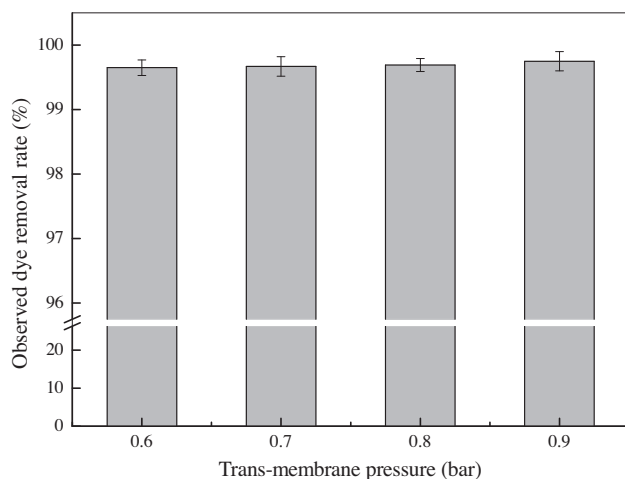


Fig. 5. Effect of TMP on the steady observed dye removal rate of the submerged NF system filtrated with textile effluent under circulation model at 25.0°C.

Table 3

Observed dye removal rate under different VCFs for the submerged NF system filtrated with textile effluent at 25.0°C and TMP of 0.8 bar

VCF	1.0	2.0	3.0	4.0
Observed dye removal rate (%)	99.82 ± 0.09	99.87 ± 0.08	99.84 ± 0.10	99.89 ± 0.08

changes slightly and still remains higher than 99.8% even under a VCF of 4.0. The results reveal that high color removal efficiency can be achieved by the submerged NF system in concentrating textile effluent, and submerged filtration employing NF membrane can be effectively used to concentrate textile wastewater with high permeate quality.

### 3.3. Permeate flux

The time-dependent average permeate fluxes of the submerged NF filtration system operated under circulation model at different TMPs are shown in Fig. 6, which clearly demonstrates that the average permeate flux under each TMP decreases continuously with the filtration time and reaches to a steady value after 30 h. The average permeate flux is declined by about 11.5, 14.5, 16.8 and 18.6% under the TMP of 0.6, 0.7, 0.8 and 0.9 bar, respectively, due to the fouling of the membrane resulted from the deposition and adsorption of dye molecules and other substances on the membrane surface, which is enhanced under

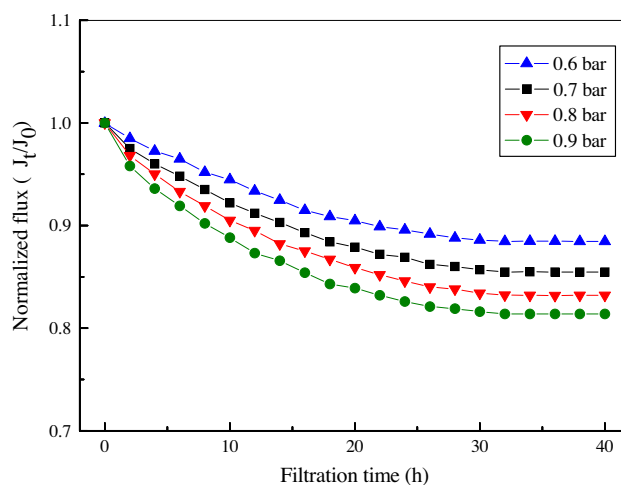


Fig. 6. Changes of normalized flux ( $J_t/J_0$ ) with filtration time for the submerged NF system filtrated with textile effluent under circulation model at the TMP of 0.6 (▲), 0.7 (■), 0.8 (▼) and 0.9 (●) bar, respectively.  $J_0$  is the initial permeate flux while  $J_t$  is the permeate flux of filtration time  $t$ .

higher TMP and can be clearly demonstrated by comparing the FE-SEM images (Hitachi S-4800, Japan) of the surfaces of the membranes employed in the experiment before and after filtration (Fig. 7).

The steady fluxes of the fouled membrane ( $J_{ws}$ ) operated under the circulation model under different

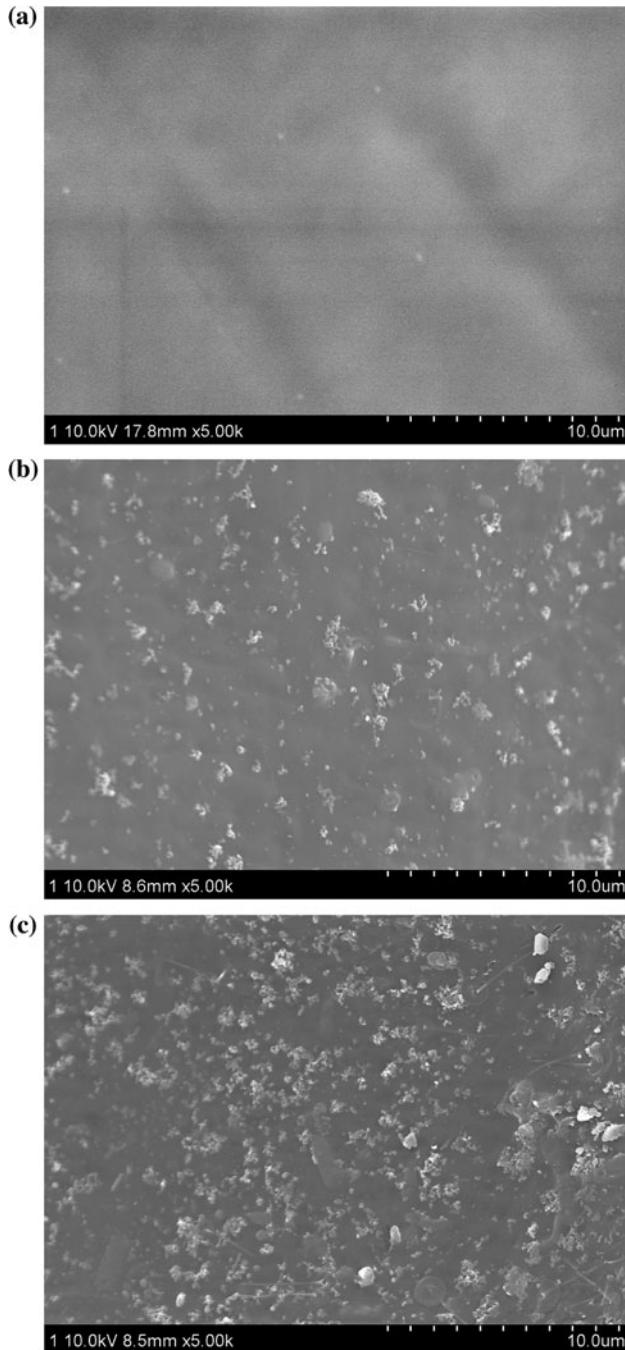


Fig. 7. FE-SEM images of the surfaces of (a) the fresh membrane, (b) the membrane filtrated under 0.6 bar, and (c) the membrane filtrated under 0.9 bar.

Table 4

Permeate fluxes  $J_{wi}$ ,  $J_{ws}$ , and  $J_{wc}$  and water flux recovery rate under different TMPs for the submerged NF system filtrated with textile effluent under circulation model at 25.0°C

TMP (bar)	$J_{wi}$ ( $l/m^2$ h)	$J_{ws}$ ( $l/m^2$ h)	$J_{wc}$ ( $l/m^2$ h)	$J_{wc}/J_{wi}$
0.6	6.50	5.75	6.29	0.968
0.7	7.60	6.50	7.32	0.963
0.8	8.64	7.20	8.30	0.961
0.9	9.70	7.90	9.30	0.959

Note:  $J_{wi}$  = pure water flux of the fresh membrane,  $J_{ws}$  = steady flux of the fouled membrane and  $J_{wc}$  = pure water flux of the water-cleaned membrane.

TMPs are presented in Table 4, which also shows the pure water fluxes of the fresh membrane ( $J_{wi}$ ) and the cleaned membrane ( $J_{wc}$ ). It can be seen from the table that, the steady state permeate flux increases with increasing TMP, while the reverse is true for the water recovery rate ( $J_{wc}/J_{wi}$ ), which declines with TMP. The water permeability of the fouled membrane obtained from the measured  $J_{ws}$  for the submerged NF system is about 9.6, 9.3, 9.0 and 8.81/ $m^2$  h bar under the TMP of 0.6, 0.7, 0.8 and 0.9 bar, respectively. The decline of water permeability is attributed to the enhanced membrane fouling on membrane surface under higher TMP, which results in an increase in the resistance to water permeation.

The change of steady permeate flux of the submerged NF system with VCF operated under the TMP of 0.8 bar is illustrated in Fig. 8, which also presents

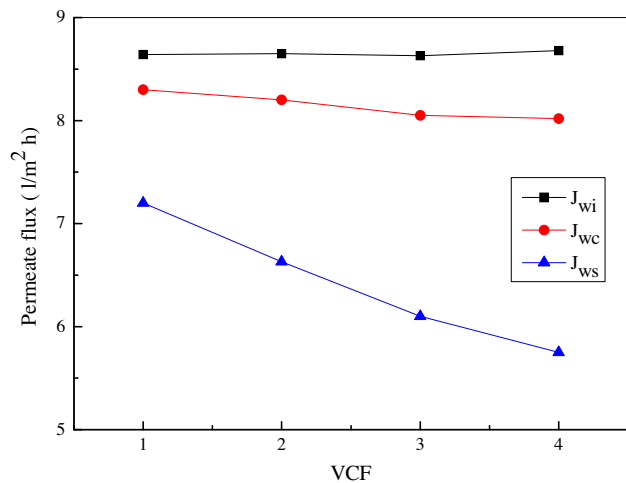


Fig. 8. Changes of fluxes  $J_{wi}$ ,  $J_{ws}$ , and  $J_{wc}$  with VCF for the submerged NF system filtrated with textile effluent under the TMP of 0.8 bar and 25.0°C.

the pure water fluxes of the fresh and water-cleaned membranes. What is apparent from the graph is that, as the VCF increases from 1.0 to 4.0, the steady permeate flux decreases progressively from about 7.20 to 5.751/m<sup>2</sup>h. The flux recovery rate of the filtrated membrane after cleaning with pure water ( $J_{wc}/J_{wi}$ ) is about 96.1, 94.7, 93.2 and 92.3% under the VCF of 1.0, 2.0, 3.0 and 4.0, respectively. The decline of water flux is due to the formation of denser fouling layer on the membrane surface under higher VCF, while the decrease in water flux recovery rate is attributed to the enhanced formation of hydraulically irreversible fouling layer, which cannot be physically removed.

### 3.4. Permeation resistance

The hydraulic resistance of fresh (clean) membrane ( $R_m$ ) was calculated from the measured pure water flux ( $J_{wi}$ ) under certain TMP through the following equation [28]:

$$J_{wi} = \frac{\text{TMP}}{\mu_w \times R_m} \quad (4)$$

where  $\mu_w$  is the water viscosity.

The hydraulic resistance of the fouling layer ( $R_f$ ) was calculated from the measured steady permeate flux ( $J_{ws}$ ) of the fouled membrane in filtration wastewater under certain TMP by adopting the resistance-in-series model through the following equation [29]:

$$J_{ws} = \frac{\text{TMP} - \Delta\Pi}{\mu_w(R_m + R_f)} \quad (5)$$

where  $\Delta\Pi$  is the trans-membrane osmotic pressure difference, which can be ignored by considering the facts that the electrolyte concentration difference between the feed and permeate conductivity is very little (as illustrated in Fig. 3), and the dye concentration in feed is very dilute [18,30].

The hydraulic resistance of the fouling layer is composed of two resistances in series:

$$R_f = R_{fr} + R_{fir} \quad (6)$$

where  $R_{fr}$  and  $R_{fir}$  are the hydraulically reversible and irreversible resistances of the fouling layer, respectively. The hydraulically reversible resistance, which is mainly due to the deposition of dyes and other foulants on membrane surface, will disappear after ceasing filtration and water washing. The hydraulically irreversible resistance, which is mainly due to the adsorption of dyes onto both the membrane surface and the inner surface of membrane pores, will

remain even after ceasing filtration and water cleaning [31].

Therefore, the permeate flux of pure water of the cleaned membrane ( $J_{wc}$ ) under certain TMP was then used to calculate the hydraulically irreversible resistance of the fouling layer ( $R_{fir}$ ) through the following equation:

$$J_{wc} = \frac{\text{TMP}}{\mu_w \times (R_m + R_{fir})} \quad (7)$$

The changes of the calculated hydraulic resistances with TMP for the submerged NF system operated under circulation model are illustrated in Fig. 9. As the TMP increase from 0.6 to 0.9 bar, the hydraulic resistance of fresh membrane  $R_m$ , as can be expected, remains almost constant, the hydraulic resistance of the fouling layer ( $R_f$ ) increases progressively from  $0.49 \times 10^{13}$  to  $0.85 \times 10^{13} \text{ m}^{-1}$  due to the increase in the hydraulically reversible resistance of the fouling layer ( $R_{fr}$ ) resulting from the enhanced deposition of foulants on membrane surface under higher TMP, since the hydraulically irreversible resistance of the fouling layer ( $R_{fir}$ ) increases slightly from  $0.13 \times 10^{13}$  to  $0.16 \times 10^{13} \text{ m}^{-1}$ . The contribution of  $R_f$  to the total hydraulic resistance to permeation ( $R_m + R_f$ ) is about 11.6, 14.4, 16.7 and 18.5%, under the TMP of 0.6, 0.7, 0.8 and 0.9 bar, respectively, indicating that the submerged NF system possesses good anti-fouling property.

The hydraulic resistances under different VCFs for the submerged NF system operated under the TMP of 0.8 bar are summarized in Table 5. One can find from the table that both the hydraulically reversible ( $R_{fr}$ )

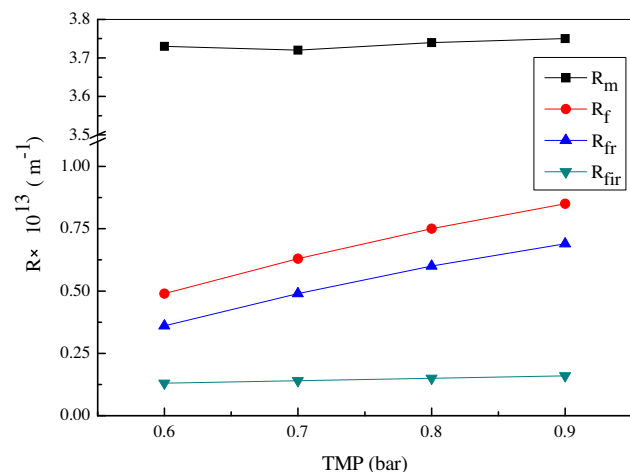


Fig. 9. Changes of hydraulic resistances  $R_m$ ,  $R_f$ ,  $R_{fr}$  and  $R_{fir}$  with TMP for the submerged NF system filtrated with textile effluent under circulation model at 25.0°C.

Table 5

Hydraulic resistances  $R_m$ ,  $R_f$ ,  $R_{fr}$  and  $R_{fir}$  under different VCFs for the submerged NF system filtrated with textile effluent under the TMP of 0.8 bar and 25.0 °C

VCF	$R_m \times 10^{13}$ ( $m^{-1}$ )	$R_f \times 10^{13}$ ( $m^{-1}$ )	$R_{fr} \times 10^{13}$ ( $m^{-1}$ )	$R_{fir} \times 10^{13}$ ( $m^{-1}$ )
1.0	3.74	0.75	0.60	0.15
2.0	3.73	1.16	0.95	0.21
3.0	3.75	1.55	1.28	0.27
4.0	3.73	1.89	1.58	0.31

Notes:  $R_m$ =hydraulic resistance of the fresh membrane,  $R_f$ =hydraulic resistance of the fouling layer,  $R_{fr}$ =hydraulically reversible resistance of the fouling layer,  $R_{fir}$ =hydraulically irreversible resistance of the fouling layer.

and irreversible resistances ( $R_{fir}$ ) of the fouling layer increase with the increase in VCF due to the enhanced membrane fouling on the membrane surface under higher VCF. Additionally, it can also be obtained from the table that, the contribution of the hydraulically reversible resistance of the fouling layer ( $R_{fr}$ ) to the total fouling resistance ( $R_f = R_{fr} + R_{fir}$ ) is about 80.0, 81.9, 82.6 and 83.6% at the VCF of 1.0, 2.0, 3.0 and 4.0, respectively. The higher value of  $R_{fr}/R_f$  reveals that most of the foulants were loosely deposited on the membrane surface during filtration and the interaction between the dye molecules and membrane surface was relatively weak.

#### 4. Conclusions

The removal of reactive dye Reactive Black 5 from textile effluent through submerged filtration using hollow fiber NF membrane has been investigated in this study. Negatively charged hollow fiber composite NF membrane with a MWCO of about 760 Da could effectively remove the dye of Reactive Black 5 from textile effluent through submerged filtration. The membrane retained the electrolytes presented in the effluent to a much low extent, so that the submerged NF system could be operated under a low suction pressure.

Under circulation model, as the filtration time prolonged, the permeate flux of the submerged NF system decreased while the dye removal rate ascended and then both reached to a steady value after a certain period. The permeability of the submerged NF system decreased with TMP, while the dye removal rate remained nearly constant.

VCF affected the water flux but had less effect on color removal efficiency. The permeability of the system declined with the increase in VCF. Steady flux of 5.751/m<sup>2</sup> h and dye removal rate of higher than 99.8% could be achieved by the submerged NF system in

filtration textile wastewater under the TMP of 0.8 bar and VCF of 4.0. Furthermore, the submerged NF system possessed good antifouling property and high water cleaning efficiency. Finally, it should be pointed out that the submerged NF system would not be normally operated if the membrane used retains the electrolytes presented in the feed solution to a great extent.

#### Acknowledgments

The authors gratefully acknowledge the financial support by the National Nature Science Foundation of China (NNSFC) (Grant No. 21276242), the National High-tech R&D Program of China (863 Program) (No. 2012AA03A601), Zhejiang Provincial Key Innovation Team (No. 2010R50038) and Innovation Fund Program For Graduate Student of Zhejiang Sci-Tech University (Grant No. YCX12005).

#### References

- [1] H. Zolliger, Color chemistry-syntheses, properties, and applications of organic dyes and pigments, third ed. Verlag Helvetica Chimica Acta, Wiley-VCH, Zürich, 2003.
- [2] E. Forgacs, T. Cserhati, G. Oros, Removal of synthetic dyes from wastewaters: A review, *Environ. Int.* 30 (2004) 953–971.
- [3] G. Tchobanoglous, F.L. Burton, H.D. Stensel, *Wastewater Engineering: Treatment and Reuse*, fourth ed., McGraw Hill, New York, NY, 2003.
- [4] N. Thinakaran, P. Panneerselvam, P. Baskaralingam, D. Elango, S. Sivanesan, Equilibrium and kinetic studies on the removal of Acid Red 114 from aqueous solutions using activated carbons prepared from seed shells, *J. Hazard. Mater.* 158 (2008) 142–150.
- [5] M. Belhachemi, F. Addoun, Adsorption of congo red onto activated carbons having different surface properties: Studies of kinetics and adsorption equilibrium, *Desalin. Water Treat.* 37 (2012) 122–129.
- [6] M.T. Sulak, H.C. Yatmaz, Removal of textile dyes from aqueous solutions with eco-friendly biosorbent, *Desalin. Water Treat.* 37 (2012) 169–177.
- [7] I. Khouni, B. Marrot, P. Moulin, R.B. Amar, Decolorization of the reconstituted textile effluent by different process treatments: Enzymatic catalysis, coagulation/flocculation and nanofiltration processes, *Desalination* 268 (2011) 27–37.
- [8] İ.A. Şengil, A. Özdemir, Simultaneous decolorization of binary mixture of blue disperse and yellow basic dyes by electrocoagulation, *Desalin. Water Treat.* 46 (2012) 215–226.
- [9] G. McMullan, C. Meehan, A. Conneely, N. Kirby, T. Robinson, P. Nigam, Microbial decolourisation and degradation of textile dyes, *Appl. Microbiol. Biotechnol.* 7 (2001) 56–81.
- [10] G. Aggelis, C. Ehalotis, F. Nerud, I. Stoychev, G. Lyberatos, G.I. Zervakis, Evaluation of white-rot fungi for detoxification and decolorization of effluents from the green olive debittering process, *Appl. Microbiol. Biotechnol.* 59 (2002) 353–360.
- [11] P. Kumar, T.T. Teng, S. Chand, K.L. Wasewar, Fenton oxidation of carpet dyeing wastewater for removal of COD and color, *Desalin. Water Treat.* 28 (2011) 260–264.
- [12] K. Turhan, I. Durukan, S.A. Ozturkcan, Z. Turgut, Decolorization of textile basic dye in aqueous solution by ozone, *Dyes Pigm.* 92 (2012) 897–901.
- [13] N.K. Daud, U.G. Akpan, B.H. Hameed, Decolorization of Sunzol Black DN conc. in aqueous solution by Fenton oxidation process: Effect of system parameters and kinetic study, *Desalin. Water Treat.* 37 (2012) 1–7.



- [14] U.G. Akpan, B.H. Hameed, Parameters affecting the photocatalytic degradation of dyes using TiO<sub>2</sub>-based photocatalysts: A review, *J. Hazard. Mater.* 170 (2009) 520–529.
- [15] B.H. Hameed, U.G. Akpan, K.P. Wee, Photocatalytic degradation of Acid Red 1 dye using ZnO catalyst in the presence and absence of silver, *Desalin. Water Treat.* 27 (2011) 204–209.
- [16] R.W. Baker, *Membrane Technology and Applications*, second ed., Wiley, Chichester, 2004.
- [17] A. Akbari, S. Desclaux, J.C. Rouch, J.C. Remigy, Application of nanofiltration hollow fibre membranes, developed by photografting, to treatment of anionic dye solutions, *J. Membr. Sci.* 297 (2007) 243–252.
- [18] W.-J. Lau, A.F. Ismail, Polymeric nanofiltration membranes for textile dye wastewater treatment: Preparation, performance evaluation, transport modelling, and fouling control—A review, *Desalination* 245 (2009) 321–348.
- [19] A. Bes-Piá, B. Cuartas-Urbe, J.-A. Mendoza-Roca, M.I. Alcina-Miranda, Study of the behaviour of different NF membranes for the reclamation of a secondary textile effluent in rinsing processes, *J. Hazard. Mater.* 178 (2010) 341–348.
- [20] E. Ellouze, N. Tahri, R.B. Amar, Enhancement of textile wastewater treatment process using nanofiltration, *Desalination* 286 (2012) 16–23.
- [21] B. Van der Bruggen, M. Mänttari, M. Nyström, Drawbacks of applying nanofiltration and how to avoid them: A review, *Sep. Purif. Technol.* 63 (2008) 251–263.
- [22] M. Gander, B. Jefferson, S. Judd, Aerobic MBRs for domestic wastewater treatment: A review with cost considerations, *Sep. Purif. Technol.* 18 (2000) 119–130.
- [23] A.G. Fane, A. Yeo, A. Law, K. Parameshwaran, F. Wicaksana, V. Chen, Low pressure membrane processes doing more with less energy, *Desalination* 185 (2005) 159–165.
- [24] Y. Ye, L.N. Sim, B. Herulah, V. Chen, A.G. Fane, Effects of operating conditions on submerged hollow fibre membrane systems used as pre-treatment for seawater reverse osmosis, *J. Membr. Sci.* 365 (2010) 78–88.
- [25] S. Yu, Y. Zheng, Q. Zhou, S. Shuai, Z. Lü, C. Gao, Facile modification of polypropylene hollow fiber microfiltration membranes for nanofiltration, *Desalination* 298 (2012) 49–58.
- [26] A.I. Schafer, A.G. Fane, T.D. Waite, *Nanofiltration—Principles and Applications*, Elsevier, 2005.
- [27] E. Sahinkaya, N. Uzal, U. Yetis, F. Dilek, Biological treatment and nanofiltration of denim textile wastewater for reuse, *J. Hazard. Mater.* 153 (2008) 1142–1148.
- [28] M. Mulder, *Basic Principles of Membrane Technology*, second ed., Kluwer Academic, Boston, MA, 1996.
- [29] S. Mattaraj, W. Phimpha, P. Hongthong, R. Jiratananon, Effect of operating conditions and solution chemistry on model parameters in crossflow reverse osmosis of natural organic matter, *Desalination* 253 (2010) 38–45.
- [30] A.C. Gomes, I.C. Gonçalves, M.N. de Pinho, The role of adsorption on nanofiltration of azo dyes, *J. Membr. Sci.* 255 (2005) 157–165.
- [31] J.L. Acero, F.J. Benitez, Ana I. Leal, F.J. Real, F. Teva, Membrane filtration technologies applied to municipal secondary effluents for potential reuse, *J. Hazard. Mater.* 177 (2010) 390–398.